6.10 CENTURY-SCALE CHANGES OF BIDECADAL OSCILLATION OVER THE NORTH PACIFIC

Shoshiro Minobe*
Graduate School of Science, Hokkaido University, Japan/
Frontier Research System for Global Change/International Arctic Research Center, Alaska

Teruko Manabe and Akiko Shouji
Japan Meteorological Agency, Tokyo, Japan

1. Introduction

Recent studies have revealed that one of the most prominent earth's climate variability on decadal-centennial timescales is the bidecadal oscillation (BO) (Mann and Park, 1996; White and Cayan, 1998). The BO distributes globally, but has the largest amplitude in the central North Pacific in association with the variability of Aleutian lows (e.g., Mann and Park 1996; White and Cayan, 1998).

The BO is an interesting phenomenon by its own right, but also is important in climatic regime shifts over the North Pacific. Minobe (1999, 2000) proposed that the quasi-simultaneous phase reversal of the BO and a 50-70 year oscillation (referred to as Pacific Pentadecadal Oscillation, PPO) resulted in the three climatic regime shifts in the 1920s, 1940s and 1970s, and that the super position of the BO and PPO gives the Pacific (inter-)Decadal Oscillation, which was proposed by Mantua et al., (1997).

An interesting feature of the BO is that the amplitude and period has changed through the 20th century; Minobe (1999, 2000) analyzed large scale climate indices over the North Pacific, which are North Pacific Index (NPI) (Trenberth and Hurrel, 1994) and Pacific Decadal Oscillation Index (Mantua et al., 1997), and described that the period is about 15 years in the beginning of 20th century and have increased to 20 years from 1930-50, during which the BO amplitudes also increased. A question arises at this point. Does the BO has a constant spatial pattern in regardless with the changes in the period? In order to understand time varying structure of the BO, we have developed a Multivariate Wavelet Filter (MWF) technique.

2. Data and Method

Winter (Dec.-Feb.) SLP anomalies north of 20°N are obtained from a monthly 5°×5° gridded SLP dataset from 1899-2000 (Trenberth and Paolino 1980), and are analyzed by using MWF. We also analyze cold-season (Nov.-May) SSTs gridded from observations in newly degitized Kobe-collection (Manabe 1999) and Comprehensive Ocean-Atmosphere Data Set.

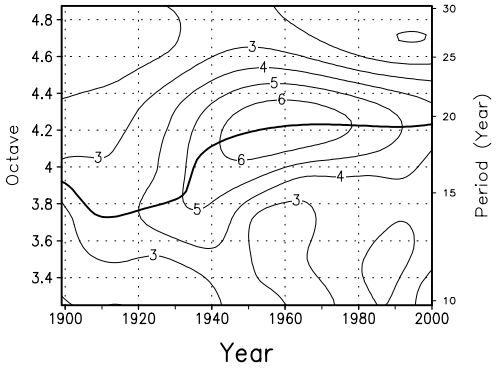

Fig. 1. Averaged absolute amplitudes of wavelet coefficients over 30-65°N, 160°E-140°W (contour) and the scale dilation parameter at the maximal amplitudes (thick curve) as a function of time.

MWF are calculated using the winter SLPs data by the following procedures. First, the wavelet transform of the wintertime SLPs are calculated at each grid point in a region from 30-65°N, 160°E-140°W (NPI region defined by Trenberth and Hurrel (1994)). Then, area averages of the absolute coefficients are obtained, and the period for the maximal averaged absolute coefficients are detected as a function of time (**Fig. 1**). The scale dilation parameter for the detected period is denoted as $a_{\max}(t)$, and the wavelet transform with respect to $a_{\max}(t)$ gives the MWF as,

$$F(x,y,t) = \frac{\sqrt{2}}{a_{\max}(t)\pi^{1/4}} \int f(x,y,t)\psi^* \left(\frac{t'-t}{a_{\max}(t)} \right) dt',$$

where x, y are the zonal and meridional distances, t the time, f the observed data, the mother wavelet, which is a Morlet wavelet in the present study, asterisk denotes the complex conjugate, F is the complex-value data filtered with the MWF, and is expressed as MWF data. It should be noteworthy that the MWF data involves two timescales, which are the oscillation timescale at the period corresponding to a_{max} and the timescale of the slow modulation of the oscillation. In

*Corresponding author address: Shoshiro. Minobe, Division of Earth and Planetary Sciences, Graduate School of Science, Hokkaido University, Sapporo 060-0810, Japan; e-mail: minobe@ep.sci.hokudai.ac.jp

order to focus on the slow modulation, we have found that it is useful to calculate time series which have relative phase with respect to a representative grid point, x_0, y_0, as follows;

$$F_r(x,y,t) = F(x,y,t)\frac{F(x_0,y_0,t)^*}{\left|F(x_0,y_0,t)\right|},$$

where F_r is the component that have the identical absolute amplitude to F, but have relative phase with respect to x_0, y_0. We refer F to as relative MWF data.

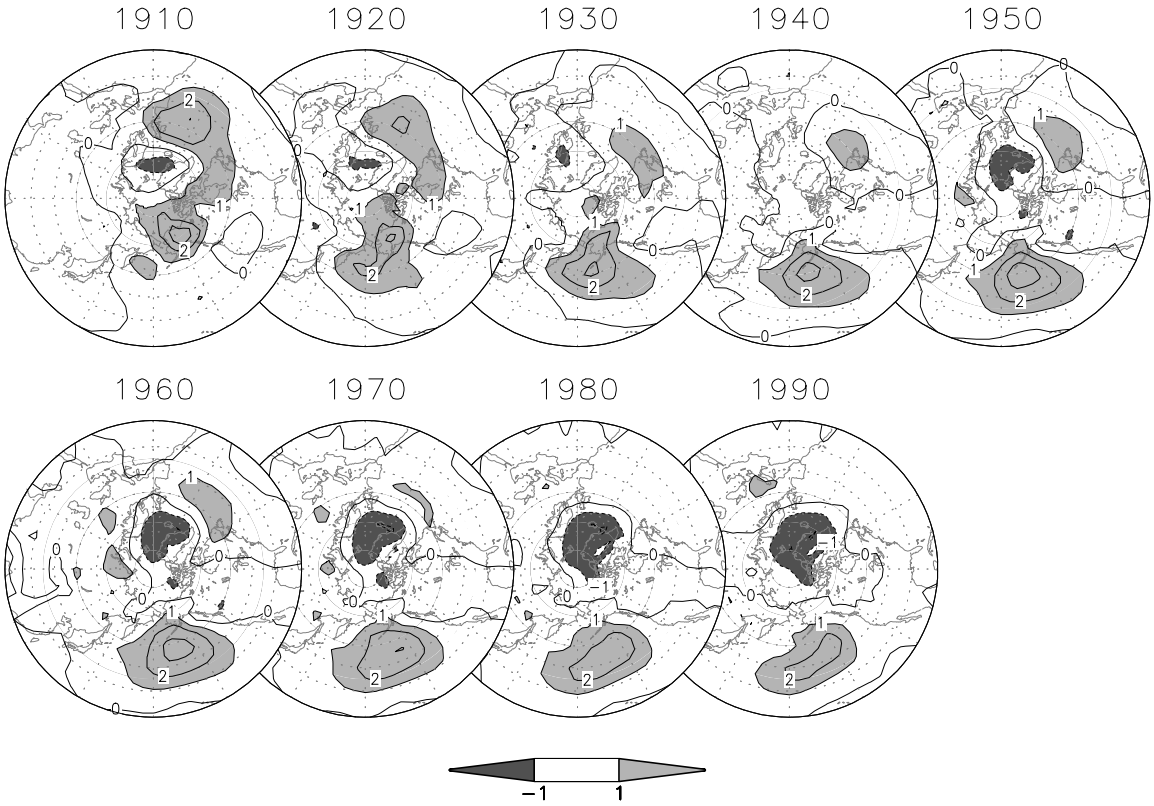

Fig. 2. Real part of the relative MWF SLPs with respect to the phase at 50°N, 165°W. Contour interval is 1 hPa.

3. Results

Figure 2 shows the real part of wintertime relative MWF SLPs with respect to 50°N 165°W from 1910 to 1980 at 10 year sampling intervals. In 1910, strong amplitudes confined over Alaska in the Pacific sector. As year progressed, the pacific action center moved into the central North Pacific from 1920 to 1950. The BO amplitude takes its maximum around 1950 with an oval pattern, and then the large amplitude region has been elongated southwest-northeastward direction accompanied by slight decrease in its amplitudes. In the Atlantic sector, the BO signatures appear as a pattern similar to the North Atlantic Oscillation. However, the amplitudes in the mid-latitudes is stronger than the high-latitude amplitudes in the early 20th century, whereas in the late 20th century, the amplitudes are larger in the Arctic region than in the mid-latitudes. The enhanced arctic amplitudes make the overall pattern resemble the Arctic Oscillation near the end of the 20th century. Consequently, the BO has migrated from the high latitude to mid-latitude in the North Pacific, and in contrast the region of the larger contributions changed from mid-latitudes to high-latitudes in the North Atlantic. These features are confirmed by analyzing complementarily EOFs for three 34-year data segments with a 10-30-year band-pass filter applied to each segments seperately (not shown).

In order to examine closely the southward migration of the BO in the North Pacific sector, we plot a latitude-time section of the SLPs averaged zonally from 160°E to 140°W by using MWF and a conventional band-pass filter with the half-power points at 10 and 30 year periods (**Fig. 3**). In the first few decades,

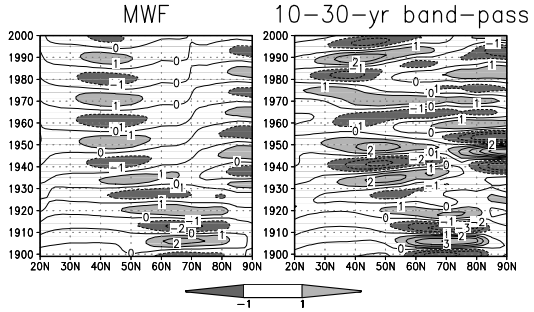

Fig. 3. Latitude-time cross section averaged over 160°E-120°W for the MWF-filtered SLPs (left) and 10-30-yr band-pass filtered SLPs (right). Contour interval is 1 hPa. The continous southward migration seen in MWF-filtered data is consistent with the result obtained by using the conventional band-pass filter.

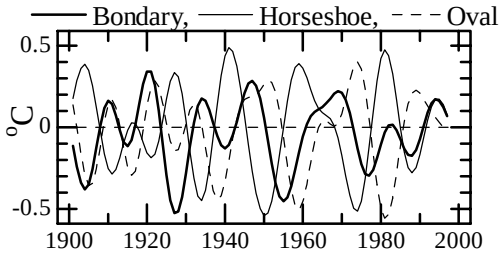

Fig. 4. 10-30 year filtered cold-season (Nov.-May) SST time series averaged over 46°-50°N, 170°-140°W (thick black curve, denoted as the border), 26-50°N, 130-110°W (thin dotted curv, denoted as the horseshoe), and 26-34N, 170E-160W (thin dashed curve, denoted as oval).

significant amplitudes are confined north of 60°N, then migrated toward the south from 1920 to 1950 with the center of the variability about 45°N in 1950. From 1950 to the present, the latitudes of the amplitude maxima shifted slowly further toward the south, and the center of the variability after 1980 locates about 40°N. Qualitatively the same features are captured by the conventional band-pass filter, but the band-pass filtered amplitudes are larger than the MWF amplitudes. The smaller amplitudes by the MWF are resulted from the narrower pass-band of it.

It is interesting to examine whether physical parameters of the atmosphere and ocean other than the SLP support or not the century-scale migration of the BO over the North Pacific. The parameter first to be examined should be SSTs, since most of the migration occurred over the central North Pacific. Unfortunately, the coverage of the available grids of the SST data is relatively poor in the early of the 20th century. Considering the availability of the SSTs and physical meanings we have chosen to examine three area averaged SSTs: 46-50°N and 170-140°W (referred to as boundary SST): 26-34°N, 170°E-160°W (oval SST): and 26-50°N, 130-110°W (horseshoe SST). The names of oval and horseshoe are come from the known BO structures in the SSTs, and boundary SST is located at the northern (southern) edge of the oval (horseshoe) SST in the central northern North Pacific.

Figure 4 shows the 10-30-year band-pass filtered time series of the boundary SST along with the oval and horseshoe SSTs. The oval and horseshoe SSTs are out of phase through the record, indicating that the overall combination of the overall and horseshoe unchanged in the 20th century. The boundary SST was used to be in-phase (out-of-phase) with the oval (horseshoe) SST in the early 20th century, but a reversed phase relationship was evident from 1980 to the present. Consequently, the oval (horseshoe) SST dominated the boundary region in the first (last) few decades, and hence the boundary between the oval and horseshoe SSTs in the first few decades was inferred to be located to the north of the present location. This result supports the southward migration of the BO observed in the SLP field.

4. Summary and Discussion

The newly developed data-analysis method, Multivariate Wavelet Filter (MWF), have successfully captured century scale changes of the BO in the SLP field over the North Pacific and North Atlantic. In the Pacific sector, the BO started from Alaska in the early 20th century, and penetrated into the North Pacific from 1920 to 1950. On the other hand, the larger BO amplitudes in the North Atlantic was found in the mid-latitudes for the first half of the century, but in high-latitudes in the latter half. The continuous migration in the Pacific sector is also observed in the latitude-time cross section of the 10-30-year band-pass filtered SLPs, which have higher temporal resolution than the MWF. The analysis of the North Pacific SSTs suggests that the boundary between the oval and horseshoe SSTs was located in the early 20th century to the north of the recent location, supporting the southward BO migration observed in the SLPs.

The spatial structure changes of the BO have substantial implications on the mechanism of the BO. Several papers has proposed that the BO arises from the air-sea interaction in the Pacific Ocean. It is noteworthy that all the mechanisms studied by these papers are more or less delay-negative feedback mechanism, though the physical processes for the delay are different from a model to another. In a delay-negative feedback model, the oscillation period is generally proportional to the delay time, and hence a wider ocean basin, which can involves a longer delay

time, may be related with a longer oscillation period. In the early 20th century, the bidecadal oscillation has a shorter timescale with mid-latitude contribution in the North Atlantic, whereas after the middle of the 20th century the mid-latitude contribution is more prominent in the Pacific basin with the longer BO timescale. Thus, the authors would like to point out the possibility that the changes of the spatial structure and timescale of the BO is related with the changes of the relative contributions between the Pacific Ocean and Atlantic Ocean. This hypothesis is, of course, at a crude speculative stage, but would be worth to be examined using air-sea coupled models in future.

Another interesting physical implication of the BO migration is for the resonance between the BO and the PPO over the North Pacific. Although the three climatic regime shifts in the 1920s, 1940s and 1970s are quite robust so that independent studies detected them (Minobe 1997; Mantua et al., 1997), it is not clear what was occurred around 1900. Minobe (1997) proposed that another regime shift occurred around 1890 based on air-temperature over mid-latitude western North America. However, the occurrence of the regime shift was not so clear, and different assessment pointed out the possibility of the regime shift around 1900 (S. Hare personal communication). The lack of a prominent regime shift around 1890-1990 may be related with the lack of the energetic BO over the central North Pacific.

From the point of view of methodology, the present results have shown that the MWF is a useful tool to know spatial structure changes corresponding to the frequency changes as far as maximal scale dilation parameters are continuously detected as a function of time. On the other hand, when maximal scale dilation parameters are discontinuous, MWF do not give physically meaningful information. However, it is not difficult to distinguish whether scale dilation parameters at the maximal wavelet amplitudes are continuous or not, when one calculates wavelet transform for a representative time series. Because wavelet transform is rapidly getting popular in studies for the atmosphere and ocean, the authors expect continuous changes of the scale-dilation parameters at the maximal wavelet amplitudes are sometimes observed in various applications of the wavelet transform. In these cases, if one wants to know whether it is related with the spatial pattern changes or not, MWF may help substantially to get some idea for the spatial changes of the signal. MWF should be used with care; MWF can have problems near the begenning and end of a record as other filtering methods, and MWF generally has smaller temporal resolution than conventional band-pass filters having a wider pass-band. These disadvantages can be overcome, by using complementaly conventional EOFs and band-pass filterings. Consequently, if one uses MWF for a proper problem with enough care, MWF would be helpful significantly.

References

Manabe, T., 1999: The digitized Kobe Collection phase I: Historical surface marine meteorological observations in the archive of the Japan Meteorological agency. *Bull. Am. Met. Soc.,* **80**, 2703-2715.

Mann, M. E., and J. Park, 1996: Joint spatiotemporal modes of surface temperature and sea level pressure variability in the Northern Hemisphere during the last century. *J. Climate,* **9**, 2137–2162.

Minobe S., 1997: A 50–70 year climatic oscillation over the North Pacific and North America. *Geophs. Res. Lett.,* **24**, 683–686.

Minobe, S., 1999: Resonance in bidecadal and pentadecadal climate oscillations over the North Pacific: Role in climatic regime shifts, *Geophys. Res. Lett.,* **26**, 855–858.

Minobe, S., 2000: Spatio-Temporal Structure of the Pentadecadal Variability over the North Pacific. *Prog. in Oceanogr.*, **47**, 99-102.

Mantua, N. J., S. R. Hare, Y., Zhang, J. M. Wallace, and R. C. Francis, A Pacific interdecadal climate oscillation with impacts on salmon production. *Bull. Am. Met. Soc. 76*, 1069–1079, 1997.

Trenberth, K. E., and D. A. Paolino, 1980: The Northern Hemisphere sea-level pressure data set: Trends, errors, and discontinuities. *Mon. Wea. Rev.* **108***,* 855–872.

Trenberth, K. E., and J. W. Hurrell, 1994: Decadal atmosphere-ocean variations in the Pacific. Climate Dynamics 9, 303-319.

White, W. B. and D. R. Cayan, 1998: Quasi-periodicity and global symmetries in interdecadal upper ocean temperature variability. *J. Geophys. Res.,* **103** (*C10*) , 21335–21354.